Verification Experiments with an Isopycnal Coordinate Ocean Model

NEIL M. BOGUE*, RUI XIN HUANG AND KIRK BRYAN

Geophysical Fluid Dynamics Laboratory/NOAA, Princeton University, Princeton, NJ 08542

4 April and 14 November 1985

ABSTRACT

The approximate conservation of density along trajectories in the upper thermocline, indicated by the observed distribution of water mass properties, suggests that isopycnal coordinates would provide a more economical framework than conventional Eulerian coordinates. An approximate analytic solution for a wind-driven circulation in a reduced gravity model is used as a prototype for testing a numerical model based on isopycnal coordinates. The numerical solutions are successful in reproducing the outcropping pattern of the analytic solutions. The application of the flux-corrected transport algorithm significantly reduces implied diffusivity relative to a first-order donor cell scheme.

1. Introduction

Much of our present understanding of ocean circulation is based on the historical file of subsurface temperature and salinity measurements collected with great effort over a period of many years. The idea of air masses was originally introduced to describe atmospheric circulation, but the concept turned out to have limited usefulness due to the rapidity with which nonadiabatic processes change temperature and moisture content along air trajectories. In the oceans, on the other hand, measurements indicate that temperature and salinity tend to be conserved for thousands of kilometers downstream of a water mass source region (e.g., a review by Reid, 1981). Thus oceanographers have found the parallel concept of water masses extremely useful. Geochemical tracers add to the specification of water masses and in some cases provide a clock, indicating elapsed time since formation. Approximate conservation does not imply that mixing across isopycnals is not an important process, and may even be dominant locally. Examples of regions where mixing across the time-averaged isopycnals is important are the surface mixed layer, near the ocean bottom, and at the equator.

A useful model of the ocean circulation must be able to simulate a large scale flow that is nearly isopycnal in the main thermocline and handle the local regions where mixing takes place. In a numerical model based on fixed Eulerian coordinates, this requirement is difficult to achieve without using extremely high resolution. It would appear that a semi-Lagrangian coordinate system based on isopycnal surfaces is a more natural and economical way to model quasi-isopycnal flows. Of course, any semi-Lagrangian scheme will involve much more complicated boundary conditions than a conventional scheme. The question is whether the advantages outweigh the added complexity that an isopycnal scheme entails. This important question remains open.

Important pioneering work on isopycnal coordinates has been carried out by Bleck (1978), Bleck and Boudra (1981) and Schopf and Cane (1983) who have overcome many of the technical difficulties involved. The present calculation uses their work as a starting point. The particular example that Bleck and Boudra use to illustrate their method is a rather complex wind-driven circulation with unstable mesoscale eddies, a regime previously explored only with quasi-geostrophic models. Our study attempts to verify the model on a much simpler case for which an approximate analytic solution is available. Our test is less ambitious than that of Bleck and Boudra, but we hope it will be useful in terms of the simpler framework it provides.

Mesinger and Arakawa (1976) have provided a very basic analysis of different finite difference formulations of the linearized shallow water equations. Since the linearized version of even complex multi-layered models can be reduced to shallow water equations for each vertical mode, their analysis is much more general than it first appears. The Bleck and Boudra (1981) model is based on what Mesinger and Arakawa refer to as the "C" grid. In this case, the pressure is defined in the center of each square of a chess board and the normal velocity components are specified at the midpoint of each side of the square. Another formulation is the "B" grid, in which the pressure is also specified at the center of each square but both of the horizontal velocity components are specified at each of the four

* Present affiliation: Honeywell Marine Systems, Seattle, WA 98103.

corner points. The difference between the two grids may seem trivial, but there are important differences in the group velocities of gravity waves simulated by the "B" and "C" grids when the Rossby radius of deformation is only marginally resolved by the grid spacing. Batteen and Han (1981) demonstrate the advantages of the "B" grid in a large-scale ocean circulation model. In an eddy resolving model, the grid size must already be fine enough to simulate nearly isopycnal flow, as shown in some recent calculations by Cox (1985).

Thus we envision that an isopycnal coordinate system will be most useful for models in which mesoscale eddies do not appear explicitly. There is a rapidly expanding data base for transient tracers in the ocean. Measurements suggest that a primary pathway of these transient tracers from the surface to the main thermocline is along isopycnal surfaces. A model formulated in terms of isopycnal coordinates would seem ideally suited for simulating the transient tracer events in which a tracer is introduced at the surface and moves slowly downward over several decades. For isopycnal models to be useful, their basic behavior must be understood, and this idea motivates the rather simple calculations of this study.

2. The analytic model

The original models of a wind-driven ocean circulation in a closed basin (see Veronis, 1981, for a review) were based on linearized, steady state, shallow water equations with simple closure schemes to represent friction. These models could be interpreted as representing an active surface layer of the ocean, underlaid by a deep abyssal layer at rest. Welander (1966) generalized this model by allowing the upper layer to have a variable depth, but retained the linearized form of the momentum equations. Parsons (1969) extended Welander's model by allowing depth variations large enough for outcropping to occur. Although there are many difficulties in extending Parsons's results to a continuously stratified model, the outcropping mechanism in his solution provides one of the simplest explanations of separation of the western boundary current in subtropical gyres. The simulation of separation in numerical solutions by Bryan (1963) or Holland and Lin (1975) is fundamentally different, depending on inertial effects in the equation of motion.

Parsons's model is in Cartesian coordinates on the beta-plane. The domain is given by $0 < x < 1$, $0 < y < 1$. Friction is specified as a simple drag, transferring momentum from the active layer to the deep, motionless layer below. The interface is displaced to exactly compensate for the pressure variations in the active layer. Motion is forced by a zonally symmetric wind stress. The nondimensional equations of the model are

$$f\mathbf{k} \times D\mathbf{u} = -D\nabla D + \lambda\tau - \epsilon\mathbf{u} \tag{2.1}$$

$$\nabla \cdot (D\mathbf{u}) = 0. \tag{2.2}$$

In (2.1) and (2.2), $\mathbf{u}$ is the horizontal velocity, D is the depth of the active layer, f and τ are the nondimensional forms of the Coriolis parameter and wind stress, respectively, and $\mathbf{k}$ is the unit vector in the vertical direction. The component of $\mathbf{u}$ normal to the boundary is zero.

The value of λ is a measure of wind forcing, while ϵ is a measure of the frictional drag. In addition, there is another parameter, R_s, which may be thought of as a Rossby number. Finally, γ is a measure of the variation of rotation over the domain. In terms of the dimensional parameters given in Table 1,

$$\left.\begin{aligned} \lambda &= LW/g'\rho_0 d^2 \\ \epsilon &= K/L\beta d \\ R_s &= g'd/L^4\beta^2 \\ \gamma &= f_0/L\beta \end{aligned}\right\}. \tag{2.3}$$

A brief explanation of the outcropping mechanism of the model is in order. Consider a subtropical gyre driven by a simple sinesoidal wind that is independent of x, thus the x-component of (2.1),

$$-fvD = -D\partial_x D - \lambda \cos\pi y. \tag{2.4}$$

Note that friction is neglected in (2.4). This approximation can be justified since friction is negligible in the interior and only important in the boundary current for the downstream component. Integrating from some point x to the eastern boundary,

$$-2f\int_x^1 Dv\,dx = -(h_E^2 - D_w^2) - 2\lambda(1 - x)\cos\pi y \tag{2.5}$$

where h_E and h_w are the depths at the eastern boundary and western boundary, respectively. At the western boundary, continuity requires that the left-hand side of (2.5) vanishes.

$$h_E^2 - D_w^2 = -2\lambda \cos\pi y. \tag{2.6}$$

For $0 < y < \frac{1}{2}$, the displacement at the western boundary will be larger than d, but in the upper northern part, $\frac{1}{2} < y < 1$, there will be a critical point for large lambda where D_w will vanish.

$$h_E^2 = -2\lambda \cos\pi y_c \tag{2.7}$$

TABLE 1. Dimensional parameters of the model.

L	Scale of the basin
W	Amplitude of the wind stress
g'	Reduced gravity
ρ_0	Reference density
d	At rest thickness of the upper layer
K	Drag coefficient
f_0	Coriolis parameter
β	Rate of change of Coriolis parameter with latitude

At this critical point separation takes place. For $y > y_c$,

$$h_E^2 = -2\lambda(1 - X)\cos\pi y \tag{2.8}$$

where X is the longitude of separation. The value of h_E can be calculated from the interior solution based on the global constraint that

$$\iint h dx dy = 1. \tag{2.9}$$

The neglect of boundary layers in calculating h_E from (2.9) limits the calculation of the point of separation to an accuracy of $O(\epsilon)$.

Several investigators have generalized Parsons' work. Kamenkovich and Reznik (1972) discussed the case where motion is allowed in the lower layer. Veronis (1973) extended the model to the world ocean. More recently, Huang (1984) has discussed similar models in a two-gyre setting over a large range of forcing conditions.

3. The numerical model

The numerical model used in this study solves a diagnostic form of (2.1) and the time-dependent form of (2.2), where time is scaled by $(L\beta)^{-1}$. All features of the model (i.e., basin size, boundary conditions, forcing) are the same as in the analytic case. No explicit lateral viscosity or diffusivity terms are included. Following Bleck (1982), the flux-corrected transport (FCT) algorithm of Boris and Book (1973) as generalized by Zalesak (1979) is used to treat the advection of layer thickness. The FCT algorithm seeks to preserve large gradients without introducing under- and overshoots that arise from second and higher order schemes. This is accomplished by computing the layer thickness at each point using a linear combination of mass fluxes computed by first and second order schemes in the particular version of the algorithm we have used in this study. An implicit lateral diffusion is introduced whenever the first order fluxes are employed. To facilitate the description of the numerical scheme we define the following operators:

$$\delta_x(\ ) = [(\ )_{i+1/2} - (\ )_{i-1/2}]/\Delta \tag{3.1}$$

$$\overline{(\ )}^x = [(\ )_{i+1/2} + (\ )_{i-1/2}]/2. \tag{3.2}$$

The subscript i denotes the position of grid points in the x-direction, and Δ is the distance between grid points. The U and V are transports, hu and hv, in the active layer, and α is a weighting coefficient between zero and unity. The superscript $n + 1$ denotes the predicted time step. The superscript n is understood except when another superscript is specified. Using this notation the Mesinger and Arakawa (1976) "B" form of the model given in (2.1) and (2.2) is

$$\epsilon u^{n+1} = -D\delta_x\bar{D}^y + \tau^x + f[\alpha V^{n+1}(1 - \alpha)V] \tag{3.3}$$

$$\epsilon v^{n+1} = -D\delta_y\bar{D}^x - f[\alpha U^{n+1}(1 - \alpha)U] \tag{3.4}$$

$$D^{n+1} = D + \Delta t\ \mathrm{FCT}(u, v, D). \tag{3.5}$$

The FCT algorithm is indicated symbolically rather than written out in detail. The FCT algorithm insures that (3.5) will be of second order accuracy in areas free of strong gradients, but where gradients do exist they will be preserved over as few as two grid points. Any initially positive definite quantity will remain positive, and α is chosen to be $\frac{2}{3}$.

The grid is a checkerboard pattern with the depth defined in the center of squares and the two velocity components defined at the corners. The boundary coincides with the position of velocity points so that the condition of no normal flow is specified exactly. At the boundary the gradient of depth, which is needed to calculate the presure force, is extrapolated from adjacent interior points. The maximum time-step permitted by the Courant-Lewy-Friedrichs condition was used in the thickness prediction (3.5).

4. Experiments

A series of experiments was performed to test the numerical model's ability to reproduce the solutions given by Parsons (1969). In particular, we are interested in qualitative comparisons in the region where the layer interface intersects the sea surface and quantitative comparisons in the basin interior. The model has a 80 × 80 grid mesh with a grid spacing equal to 40 km and the central latitude at 35°N. The nondimensional parameters for different cases shown in Figs. 1 and 2 are specified in Table 2.

a. The first supercritical state

When lambda is larger than a critical value, the lower layer outcrops (Parsons, 1969). Figure 1 shows the nondimensional upper-layer depth. The at-rest depth of the upper layer is 1.0. The case shown in Fig. 1a was numerically integrated to an equilibrium state. Thin solid lines indicate the depth of the upper layer in the numerical solution, the heavy solid line is the outcropping line for the analytical solution, and the dashed lines are the analytic solution. The two solutions are constrained to have the same lambda. One source of discrepancy is the lack of a western boundary region in the analytic solution. Actually, the analytical solu-

TABLE 2. Nondimensional parameters of the different case shown in Figs. 1 and 2.

Figure	λ	ϵ	R_s	$f_0/\beta L$
1(a)	0.36	0.01	1.64×10^{-4}	1.4
1(b)	0.60	0.06	1.64×10^{-4}	1.4
1(c)	0.60	0.02	1.64×10^{-4}	1.4
1(d)	0.60	0.02	1.64×10^{-4}	1.4
2	9.60	0.06	0.46×10^{-4}	1.4

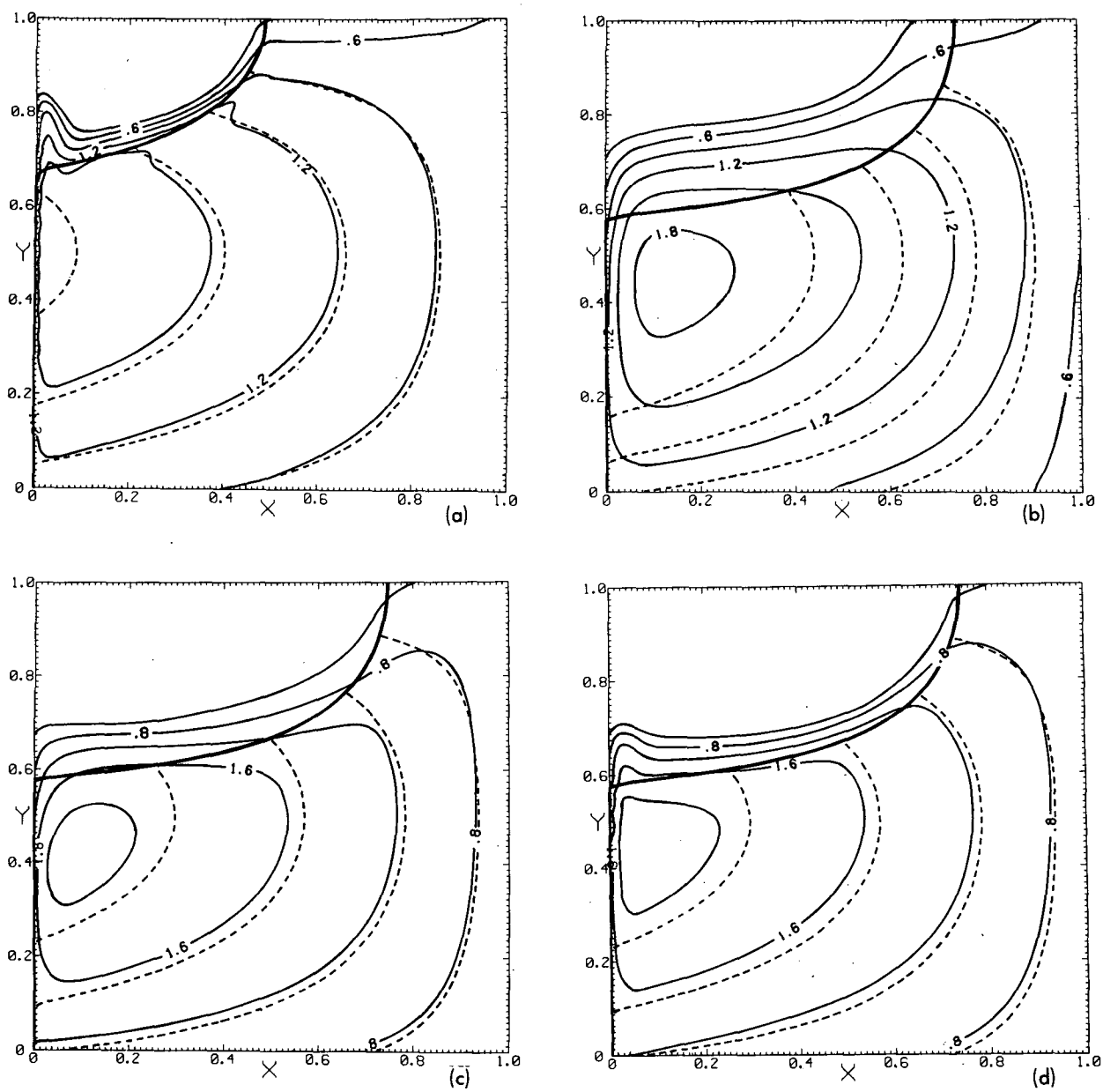

FIG. 1. Nondimensional upper-layer thickness. Numerical results are shown in thin solid lines, analytical results in dashed lines, outcropping lines for analytical solutions are in heavy solid lines. (a) $\lambda = 0.36$, $\epsilon = 0.01$, FCT code; (b) $\lambda = 0.60$, $\epsilon = 0.06$, FCT code; (c) $\lambda = 0.60$, $\epsilon = 0.02$, Donner-cell code only; (d) $\lambda = 0.60$, $\epsilon = 0.02$, FCT code.

tion drawn in Fig. 1 corresponds to the case with ϵ being infinitely small, thus all boundary currents are infinitely narrow. The numerical solution is shallower than the analytic solution at the western wall and extends beyond the outcropping line after separation. Another discrepancy arises at the eastern boundary. In the analytic solution, the depth is assumed to be uniform along the entire boundary. The numerical results maintain a meridional gradient in the upper to maintain the following balance:

$$\epsilon V = D\partial_y D. \tag{4.1}$$

In practice the difference is slight. Overall, the analytical solution is deeper in the interior to compensate for the volume missing adjacent to the outcropping line. Since the parameters for Fig. 1a make the outcropping region relatively narrow, the discrepancy in depth is also small.

An unanticipated feature of the numerical solution is the overshoot of the western boundary current beyond the separation point predicted by the Parsons

theory. The equations are of very low order and do not contain inertial effects which play a crucial role in the models of Bryan (1963) and Veronis (1966). Thus the overshooting feature is quite different from what has been obtained in previous studies. An analysis of the overshoot and a simple analytic theory are given in a separate paper (Huang, 1986).

A second case with $\lambda = 0.60$ and $\epsilon = 0.06$ is shown in Fig. 1b. It is clear that as λ increases, the outcropping zone is enlarged; as ϵ increases, the width of the boundary currents increase too. As a result, the discrepancy between the numerical and analytical solutions becomes larger.

The difference in patterns when only a first order, donor cell scheme is used to compute depths rather than the full flux corrected algorithm is dramatic. This is illustrated in Fig. 1c and 1d. In Fig. 1c, the use of the donor cell method gives a wide boundary current region outside the analytic outcropping region. The boundary current region is significantly narrower when the FCT scheme is applied for the same parameters as shown in Fig. 1d. The effect of reducing ϵ is clear by comparing Fig. 1b with 1d. Note that the narrower outcropping current gives significantly better agreement with the analytic solution in the interior, because of the global volume constraint pointed out in the previous section. Note that overshoot occurs in the western boundary current in this case, but with a smaller amplitude than in the case shown in Fig. 1a.

b. Case 2: The second supercritical state

The case in Fig. 2 corresponds to a large value of lambda, i.e., very strong wind driving or very small amounts of upper-layer water. The upper, active layer is confined to a very small pool. This is an extreme case beyond the parameter range considered by Parsons, but such cases have been discussed by Huang (1984) using a similar analytical model. In Huang's (1984) solution, the active fluid is confined to a roughly rectangular region in the lower, left-hand part of the basin. Figure 2 confirms this prediction to a certain extent. The numerical solution, however, contains a tail extending out from the outcropping line toward the eastern boundary. This phenomenon is now being investigated in connection with two-gyre circulation studies using the same model.

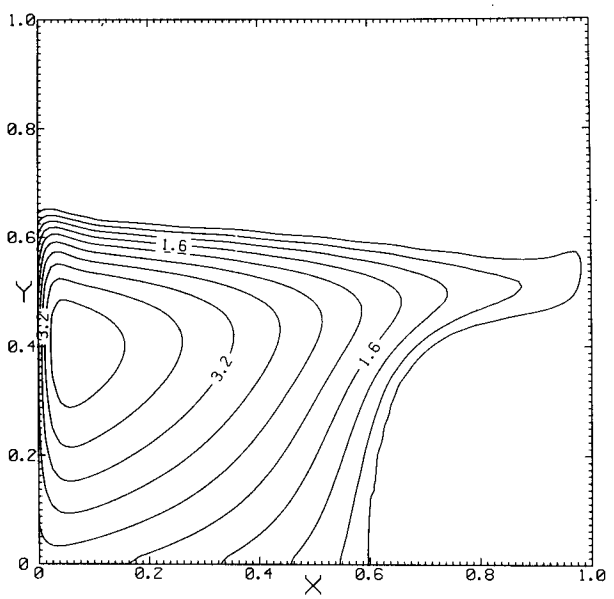

FIG. 2. Nondimensional upper-layer thickness for the second supercritical state ($\lambda = 9.6$, $\epsilon = 0.06$).

5. Discussion

The interesting mechanism for separation of the western boundary current in Parsons' (1969) model makes it an ideal analytical solution for verifying a numerical model based on isopycnal coordinates. Although this study is only concerned with a very simple reduced gravity system, it can be thought of as a prototype for much more complex multilayer models with closure schemes allowing for cross-isopycnal mixing. Cox (1985) has shown that high resolution three-dimensional models based on conventional Eulerian coordinates can simulate nearly isopycnal flow in the main thermocline. It would appear that isopycnal models would be most useful in ocean circulation models which are not able to resolve mesoscale eddies explicitly. There is a wide range of applications in air–sea interaction and transient tracer studies where models of this type are needed. With this application in mind we have replaced the "C" grid as defined by Mesinger and Arakawa (1976) in Bleck and Boudra's (1981) model with the "B" grid, a slightly different arrangement of variables in the horizontal plane. The result is a model which has better wave propagation properties in the range for which the Rossby radius of the first baroclinic mode is just barely resolved by the horizontal grid.

Our tests show agreement with Parsons's solution to within the accuracy of the approximations of the theory. Although there is no explicit horizontal diffusion in the first model, implicit diffusion can take place locally when first order differencing is used to correct errors of over- or undershooting caused by second order differencing in the transport equation. An impressive Lagrangian scheme for a reduced gravity, shallow water model has been demonstrated by Salmon (1983). Lagrangian schemes may ultimately turn out to be the most efficient transport models, but much more development is required for general applications. The present isopycnal scheme may be thought of as an intermediate model which is at least Lagrangian in the vertical, and it is possible, as Bleck and Boudra (1981) have shown, to generalize the scheme to three dimensions.

Acknowledgments. The authors are deeply grateful to G. P. Williams and R. Salmon for helpful suggestions for improving both the model and the presentation of the results. We would also like to thank P. Tunison and his staff for assistance with the figures and to M. Jackson and J. Pege for their work in final preparation of the manuscript.

REFERENCES

Batteen, M. L., and Y. J. Han, 1981: On the computational noise of finite-difference schemes used in ocean models. *Tellus,* **33,** 387–396.

Bleck, R., 1978: Simulation of coastal upwelling frontogenesis with an isopycnic coordinate model. *J. Geophys. Res.,* **83,** 6163–6172.

——, 1982: A sensitivity experiment concerning the numerical simulation of lee cyclogenesis. *ALPEX Experiment: Preliminary Scientific Results,* WMO.

——, and D. B. Boudra, 1981: Initial testing of a numerical ocean circulation model using a hybrid (quasi-isopycnic) vertical coordinate. *J. Phys. Oceanogr.,* **11,** 755–770.

Boris, J. P., and D. L. Book, 1973: Flux-corrected transport. I. SHASTA, A fluid transport algorithm that works. *J. Comput. Phys.,* **11,** 38–69.

Bryan, K., 1963: A numerical investigation of a nonlinear model of a wind-driven ocean. *J. Atmos. Sci.,* **20,** 594–606.

Cox, M. D., 1985: An eddy resolving numerical model of the ventilated thermocline. *J. Phys. Oceanogr.,* **15,** 1312–1324.

Holland, W., and L.-B. Lin, 1975: On the generation of mesoscale eddies and their contribution to the oceanic general circulation. I: A preliminary numerical experiment. *J. Phys. Oceanogr.,* **5,** 692–657.

Huang, R. X., 1984: The thermocline and current structure in subtropical/subpolar basins. Ph.D. thesis, Massachusetts Institute of Technology/Woods Hole Oceanographic Institution, WHOI-84-42, 218 pp.

——, 1986: Numerical simulation of wind-driven circulation in a subtropical-subpolar basin. *J. Phys. Oceanogr.,* **16** (in press).

Kamenkovich, V. M., and G. M. Reznik, 1972: A contribution to the theory of stationary wind-driven currents in a two-layer liquid. *Izv., Acad. Sci., USSR, Atmos. Ocean. Phys.,* (Engl. Transl.), **8,** 238–245.

Mesinger, F., and A. Arakawa, 1976: Numerical Methods Used in Atmospheric Models. GARP Publ. No. 17, WMO, 64 pp.

Parsons, A. T., 1969: A two-layer model of Gulf Stream separation. *J. Fluid Mech.,* **39,** 511–528.

Reid, J. L., 1981: On the mid-depth circulation of the World Ocean. *Evolution of Physical Oceanography.* B. A. Warren and C. Wunsch, Eds., The MIT Press, 70–110.

Salmon, R., 1983: Practical use of Hamilton's principle. *J. Fluid Mech.,* **132,** 431–444.

Schopf, P. S., and M. A. Cane, 1983: On equatorial dynamics, mixed layer physics, and sea surface temperature. *J. Phys. Oceanogr.,* **13,** 917–935.

Veronis, G., 1966: Wind-driven ocean circulation: Part II. Numerical solutions of the non-linear problem. *Deep-Sea Res.,* **13,** 31–55.

——, 1973: Model of world ocean circulation: I. Wind-driven, two layer. *J. Mar. Res.,* **31,** 228–288.

——, 1981: Dynamics of large-scale ocean circulation. *Evolution of Physical Oceangraphy.* B. A. Warren and C. Wunsch, Eds., The MIT Press, 140–183.

Welander, P., 1966: A two-layer frictional model of wind-driven motion in a rectangular oceanic basin. *Tellus,* **18,** 54–62.

Zalesak, S. T., 1979: Fully multidimensional flux-corrected transport algorithms for fluids. *J. Comput. Phys.,* **31,** 335–362.